

Vacuum amplitudes and time-like causal unitary in the loop-tree duality

The LTD Collaboration, Selomit Ramírez-Uribe ^(a,b), Andrés E. Rentería-Olivo ^(a), David F. Rentería-Estrada ^(a), Jorge J. Martínez de Lejarza ^(a), Prasanna K. Dhani ^(a), Leandro Cieri ^(a), Roger J. Hernández-Pinto ^(b), German F. R. Sborlini ^(c), William J. Torres Bobadilla ^(d), and Germán Rodrigo ^{(a)*}

^a Instituto de Física Corpuscular, Universitat de València – Consejo Superior de Investigaciones Científicas, Parc Científic, E-46980 Paterna, Valencia, Spain.

^b Facultad de Ciencias Físico-Matemáticas, Universidad Autónoma de Sinaloa, Ciudad Universitaria, CP 80000 Culiacán, Mexico.

^c Departamento de Física Fundamental e IUFFyM, Universidad de Salamanca, 37008 Salamanca, Spain.

^d University of Liverpool, Liverpool L69 3BX, United Kingdom.

(Dated: April 8, 2024)

We present the first proof-of-concept application to decay processes at higher perturbative orders of LTD causal unitary, a novel methodology that exploits the causal properties of vacuum amplitudes in the loop-tree duality (LTD) and is directly well-defined in the four physical dimensions of the space-time. The generation of loop- and tree-level contributions to the differential decay rates from a kernel multiloop vacuum amplitude is shown in detail, and explicit expressions are presented for selected processes that are suitable for a lightweight understanding of the method. Specifically, we provide a clear physical interpretation of the local cancellation of soft, collinear and unitary threshold singularities, and of the local renormalisation of ultraviolet singularities. The presentation is illustrated with numerical results that showcase the advantages of the method.

I. INTRODUCTION

In a recent paper [1], we have proposed a novel representation of differential observables at high-energy colliders that exploits the manifestly causal properties of the loop-tree duality (LTD) at higher perturbative orders and its connections with directed acyclic graph (DAG) configurations in graph theory [2–17]. This approach, dubbed LTD causal unitary, generalises the method of four-dimensional unsubtraction (FDU) [18–25] in which, unlike subtraction methods [26–67], infrared (IR) and ultraviolet (UV) singularities are locally cancelled directly between loop and tree contributions at the integrand level, while introducing relevant improvements and new features that facilitate an efficient implementation.

The central and novel ingredient of LTD causal unitary is a multiloop vacuum amplitude in the LTD representation that depends on Λ loop momenta, $\{\ell_j\}_{j=1,\dots,\Lambda}$. In LTD causal unitary, the differential contribution to the decay rate of a particle of mass m_a from the k^{th} -order in perturbation theory is given by

$$d\Gamma_a^{(k)} = \frac{d\Lambda}{2m_a} \sum_{(i_1 \dots i_n a) \in \Sigma} \mathcal{A}_D^{(\Lambda, R)}(i_1 \dots i_n a) \tilde{\Delta}_{i_1 \dots i_n a}, \quad (1)$$

and

$$d\Gamma_a^{\text{N}^k \text{LO}} = \sum_{j=0}^k d\Gamma_a^{(j)}, \quad (2)$$

where $d\Gamma_a^{\text{N}^k \text{LO}}$ denotes the differential decay rate up to (next-to)^k-leading order, and the integration measure

$$d\Lambda = \prod_{j=1}^{\Lambda-1} d\Phi_{\ell_j} = \prod_{j=1}^{\Lambda-1} \mu^{4-d} \frac{d^{d-1}\ell_j}{(2\pi)^{d-1}}, \quad (3)$$

is written in terms of the spatial components of $\Lambda - 1$ primitive loop momenta, as the spatial components of one of them are fixed by the decaying particle. A detailed derivation of the integration measure from the customary phase space is presented in Appendix A. The number of loops of the vacuum amplitude is $\Lambda = L + N - 1$, where N is the total number of external particles in LO kinematics, and L is the maximum number of loops that contribute at the k^{th} perturbative order. In Eq. (1), Σ denotes the set of all the phase-space configurations contributing at the k^{th} order, with $n \in \{m, \dots, m+k\}$, where m is the number of final-state particles in LO kinematics. For a decay process, $m = N - 1$.

The final states with n particles are then generated from residues, called phase-space residues, of a vacuum amplitude $\mathcal{A}_D^{(\Lambda)}$ on the on-shell energies of the internal propagators, $q_{i_s,0}^{(+)} = \sqrt{\mathbf{q}_{i_s}^2 + m_{i_s}^2} - i0$, where $i0$ is the original complex prescription of a Feynman propagator, \mathbf{q}_{i_s} the spacial components of the four-momentum q_{i_s} , and m_{i_s} its mass,

$$\begin{aligned} \mathcal{A}_D^{(\Lambda, R)}(i_1 \dots i_n a) &= \mathcal{A}_D^{(\Lambda)}(i_1 \dots i_n a) \\ &\quad - \mathcal{A}_{UV}^{(\Lambda)}(i_1 \dots i_n a), \end{aligned} \quad (4)$$

where

$$\mathcal{A}_D^{(\Lambda)}(i_1 \dots i_n a) = \text{Res} \left(\frac{x_a}{2} \mathcal{A}_D^{(\Lambda)}, \lambda_{i_1 \dots i_n a} \right), \quad (5)$$

with

$$\lambda_{i_1 \dots i_n a} = \sum_{s=1}^n q_{i_s,0}^{(+)} + q_{a,0}^{(+)}. \quad (6)$$

The counterterm $\mathcal{A}_{UV}^{(\Lambda)}(i_1 \dots i_n a)$ in Eq. (4) implements a local UV renormalisation. The residue at $\lambda_{i_1 \dots i_n a} = 0$ is obtained by analytically continuing the initial-state on-shell energy, $q_{a,0}^{(+)} = \sqrt{\mathbf{q}_a^2 + m_a^2} - i0$, to negative values, i.e., $q_{a,0}^{(+)} = -p_{a,0}^{(+)}$. We have defined $x_a = 2q_{a,0}^{(+)}$.

* german.rodrigo@csic.es

The last factor in Eq. (1) encodes energy conservation

$$\tilde{\Delta}_{i_1 \dots i_n \bar{a}} = 2\pi \delta(\lambda_{i_1 \dots i_n \bar{a}}), \quad (7)$$

with

$$\lambda_{i_1 \dots i_n \bar{a}} = \sum_{s=1}^n q_{i_s,0}^{(+)} - p_{a,0}^{(+)}. \quad (8)$$

The LTD causal unitary representation in Eq. (1) involves the sum over all possible phase-space residues of the vacuum amplitude. It is precisely the unitary sum over all of them that ensures that most of the unique properties of the vacuum amplitude are preserved. Specifically, the vacuum amplitude in LTD is a function of the on-shell energies and is obtained by replacing the Feynman propagators by causal propagators of the form

$$\frac{1}{\lambda_{i_1 \dots i_m}} = \left(\sum_{s=1}^m q_{i_s,0}^{(+)} \right)^{-1}. \quad (9)$$

The numerator of the vacuum amplitude is also a function of the on-shell energies and additionally of the internal masses.

Since the real part of the on-shell energies is positive by definition, the causal propagators in Eq. (9) cannot become singular. If all the on-shell energies vanish simultaneously for massless particles, the potential soft singularity is screened by the integration measure which also vanishes in this limit. As a consequence, the vacuum amplitude cannot exhibit soft or collinear singularities, and remarkably unitary threshold singularities are also absent. The absence of singularities in the vacuum amplitude, apart from UV singularities that are accounted for by the local UV counterterm, ensures that the unitary sum over the phase-space residues is also free of soft, collinear and unitary threshold singularities [1]. Therefore, the master expression for the decay rate in Eq. (1) is well defined in the four physical dimensions of the space-time, since all potential singularities locally cancel out between different phase-space residues.

The purpose of this paper is to provide a first proof-of-concept implementation of LTD causal unitary for physical processes, and to showcase its coherence and advantages in a detailed manner, especially with respect to the physical interpretation of the contributing components.

The outline of the paper is as follows. In Section II, we present explicit expressions for the phase-space residues that contribute to the decay processes $H \rightarrow q\bar{q}(g)$ and $\gamma^* \rightarrow q\bar{q}(g)$ at LO and NLO. In Section III, we construct the corresponding UV counterterms, which implement a local UV renormalisation, and discuss in detail the wave-function renormalisation and the mass renormalisation scheme. In Section IV, we consider a simplified model that has all the main properties of a NNLO calculation and is therefore suitable for presenting LTD causal unitary at NNLO in a lightweight form. In Section V, we present a numerical implementation of LTD causal unitary at NLO and NNLO based on the phase-space residues presented in Sections II to IV, and illustrate the local cancellation of unitary threshold, double- and triple-collinear/quasicollinear singularities. Finally, in Section VI we draw our conclusions and future prospects.

II. VACUUM AMPLITUDES AND DECAY RATES AT NLO

We present explicit expressions up to NLO for the decay processes $H \rightarrow q\bar{q}(g)$ and $\gamma^* \rightarrow q\bar{q}(g)$. These processes are well suited to easily illustrate all the main features of LTD causal unitary with compact analytical expressions. The kernel vacuum amplitude used to derive the total or differential decay rate, or any other physical observables, is constructed from the vacuum diagrams depicted in Fig. 1. The two-loop vacuum diagram, on the left, generates the differential expression of the decay rate at LO. The remaining three-loop diagrams contribute to the decay rate at NLO. Note that the diagram on the right and similar diagrams naturally generate selfenergy insertions in external legs. Their contribution is essential to achieve a local cancellation of all IR singularities with the real emission final-state configurations. The internal momenta are labelled as follows in terms of the loop momenta $\{\ell_s\}_{s=1,2,3}$:

$$\begin{aligned} q_1 &= \ell_1 + \ell_2, & q_2 &= \ell_1 + \ell_3, & q_3 &= \ell_1, \\ q_4 &= \ell_2, & q_5 &= \ell_2 - \ell_3, & q_6 &= \ell_3. \end{aligned} \quad (10)$$

We use the shorthand notation $\ell_{ij} = \ell_i + \ell_j$ and $\ell_{i\bar{j}} = \ell_i - \ell_j$. Nonetheless, it is worth noting that one of the advantages of the LTD representation is that it is independent of the specific labelling of the internal momenta. The momentum q_1 represents a gluon and is massless, while q_2 through q_5 are quarks or antiquarks of mass m . The momentum q_6 is either a Higgs boson or an off-shell photon. To simplify the presentation, we define $x_{i_1 \dots i_n} = \prod_{s=1}^n 2q_{i_s,0}^{(+)}$.

The two-loop dual vacuum amplitude associated to the LO decay rate has the compact form

$$\mathcal{A}_D^{(2,f)} = \frac{2g_f^{(0)}}{x_{456}} \left(\frac{|\mathcal{M}_{f \rightarrow q\bar{q}}^{(0)}|^2}{\lambda_{456}} + 2\lambda_{45\bar{6}} \right), \quad f = H, \gamma^*. \quad (11)$$

For convenience, the average factor over initial-state polarizations is included in $\mathcal{A}_D^{(2,f)}$. In this expression, we have anticipated that $|\mathcal{M}_{f \rightarrow q\bar{q}}^{(0)}|^2$ is the matrix element squared obtained with the standard approach of squaring the tree-level amplitude for $f \rightarrow q\bar{q}$ and averaging over the initial-state polarizations, where the interaction couplings and final-state colour factors are collected in the coefficient $g_f^{(0)}$,

$$g_H^{(0)} = y_q^2 C_A, \quad g_{\gamma^*}^{(0)} = (ee_q)^2 C_A, \quad (12)$$

with y_q the Yukawa coupling of the quark, e_q the quark electric charge in terms of the electric charge unit e , and the Casimir color factor $C_A = 3$.

The corresponding phase-space residue is given by

$$\mathcal{A}_D^{(2,f)}(456) \equiv \text{Res} \left(\frac{x_6}{2} \mathcal{A}_D^{(2,f)}, \lambda_{456} \right) = \frac{g_f^{(0)}}{x_{45}} \overline{|\mathcal{M}_{f \rightarrow q\bar{q}}^{(0)}|^2}, \quad (13)$$

with

$$\overline{|\mathcal{M}_{H \rightarrow q\bar{q}}^{(0)}|^2} = 2s\beta^2, \quad \overline{|\mathcal{M}_{\gamma^* \rightarrow q\bar{q}}^{(0)}|^2} = 2s \left(1 + \frac{1 - \beta^2}{d - 2} \right), \quad (14)$$

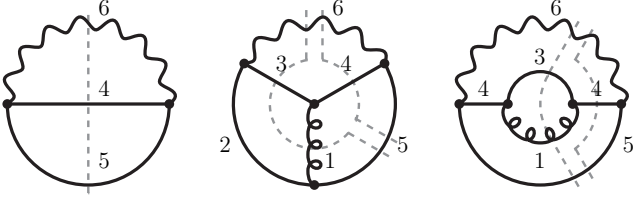


FIG. 1. The two- and three-loop vacuum diagrams generating $\gamma^* \rightarrow q\bar{q}(g)$ at LO and NLO, respectively. The gray dashed lines represent phase-space residues. Similar diagrams contribute to $H \rightarrow q\bar{q}(g)$ by substituting the photon labeled as 6 with a Higgs boson.

where $\beta = \sqrt{1 - 4m^2/s}$ is the velocity of the quark in terms of its mass m and the centre-of-mass energy squared s , and $d = 4 - 2\epsilon$ is the number of space-time dimensions in dimensional regularisation (DREG). The factor $1/x_{45}$ is, in effect, the expected factor arising from a phase space as the product of the final-state energies, whereas here it is actually generated in a natural way from the phase-space residue on the vacuum amplitude. The on-shell energy of the decaying particle is $q_{6,0}^{(+)} = \sqrt{s - i0}$, with $s = m_H^2$ for the Higgs boson decay, as we set $\ell_3 = \mathbf{0}$ in the centre-of-mass frame. The partial decay rate at LO is then given by

$$d\Gamma_{f \rightarrow q\bar{q}}^{\text{LO}} = \frac{d\Phi_{\ell_2}}{2\sqrt{s}} \mathcal{A}_D^{(2,f)}(456) \tilde{\Delta}_{45\bar{6}}. \quad (15)$$

The phase-space condition encoded by $\tilde{\Delta}_{45\bar{6}}$ imposes $q_{4,0}^{(+)} = q_{5,0}^{(+)} = q_{6,0}^{(+)}/2$ in the frame where $\ell_3 = \mathbf{0}$:

$$\tilde{\Delta}_{45\bar{6}} = \frac{\pi}{\beta} \delta\left(|\ell_2| - \frac{\beta\sqrt{s}}{2}\right). \quad (16)$$

Conservation of the three-momentum is already consistently fulfilled in the vacuum amplitude. Thus, the total decay rates at LO agree with the well-known results

$$\begin{aligned} \Gamma_{H \rightarrow q\bar{q}}^{\text{LO}} &= g_H^{(0)} \frac{\beta^3 m_H}{8\pi}, \\ \Gamma_{\gamma^* \rightarrow q\bar{q}}^{\text{LO}} &= g_{\gamma^*}^{(0)} \frac{\beta\sqrt{s}}{8\pi} \left(1 + \frac{2m^2}{s}\right). \end{aligned} \quad (17)$$

Such a LO calculation, performed through the phase-space residues of a two-loop vacuum amplitude, may seem redundant and overly complex. Yet, the benefits of the method emerge clearly at higher orders.

We now consider the three-loop vacuum amplitude acting as the kernel dual amplitude at NLO. We shall evaluate phase-space residues involving 3 and 4 external particles, which correspond to the virtual and real contributions to the decay rate at NLO. The differential decay rate at NLO is

$$\begin{aligned} d\Gamma_{f \rightarrow q\bar{q}}^{(1)} &= \frac{d\Phi_{\ell_1 \ell_2}}{2\sqrt{s}} \left[\left(\mathcal{A}_D^{(3,f,R)}(456) \tilde{\Delta}_{45\bar{6}} \right. \right. \\ &\quad \left. \left. + \mathcal{A}_D^{(3,f)}(1356) \tilde{\Delta}_{135\bar{6}} \right) + (5 \leftrightarrow 2, 4 \leftrightarrow 3) \right]. \end{aligned} \quad (18)$$

The first phase-space residue, unrenormalised, which corresponds to the interference of a one-loop with a tree-level amplitude, is given for the decay of the Higgs boson by

$$\begin{aligned} \mathcal{A}_D^{(3,H)}(456) &= \frac{g_H^{(1)}}{x_{12345}} \left[\left\{ h_D(456) \overline{|\mathcal{M}_{H \rightarrow q\bar{q}}^{(0)}|^2} \right. \right. \\ &\quad + 2(d-2)\lambda_2 \left(-\frac{\lambda_{125}\lambda_{1\bar{2}\bar{5}}}{\lambda_{13\bar{4}}} - \frac{\lambda_{12\bar{5}}\lambda_{1\bar{2}\bar{5}}}{\lambda_{134}} + 2\lambda_{1\bar{3}} \right) \\ &\quad + \lambda_1 \left((d-2) \overline{|\mathcal{M}_{H \rightarrow q\bar{q}}^{(0)}|^2} - 4s \right) \left(\frac{1}{\lambda_{23\bar{4}\bar{5}}} + \frac{1}{\lambda_{2345}} \right) \left. \right\} \\ &\quad \left. + (2 \leftrightarrow 3, 4 \leftrightarrow 5) \right], \end{aligned} \quad (19)$$

and for the decay of an off-shell photon by

$$\begin{aligned} \mathcal{A}_D^{(3,\gamma^*)}(456) &= \frac{g_{\gamma^*}^{(1)}}{x_{12345}} \left[\left\{ h_D(456) \overline{|\mathcal{M}_{\gamma^* \rightarrow q\bar{q}}^{(0)}|^2} \right. \right. \\ &\quad + 2(d-2)\lambda_2 \left(-\frac{\lambda_{125}\lambda_{1\bar{2}\bar{5}}}{\lambda_{13\bar{4}}} - \frac{\lambda_{12\bar{5}}\lambda_{1\bar{2}\bar{5}}}{\lambda_{134}} + 2\lambda_{13} \frac{d-4}{d-2} \right) \\ &\quad + \lambda_1 \left(((d-4) \overline{|\mathcal{M}_{\gamma^* \rightarrow q\bar{q}}^{(0)}|^2} - 8s) \left(\frac{1}{\lambda_{23\bar{4}\bar{5}}} + \frac{1}{\lambda_{2345}} \right) \right. \\ &\quad \left. + \frac{4\lambda_{12\bar{5}}\lambda_{1\bar{2}\bar{5}}}{\lambda_{23\bar{4}\bar{5}}} + \frac{4\lambda_{125}\lambda_{1\bar{2}\bar{5}}}{\lambda_{2345}} \right) \left. \right\} + (2 \leftrightarrow 3, 4 \leftrightarrow 5) \right], \end{aligned} \quad (20)$$

where the function $h_D(456)$ is common to both residues,

$$\begin{aligned} h_D(456) &= s(1 + \beta^2) \\ &\quad \times \left[\frac{1}{\lambda_{13\bar{4}}} \left(\frac{1}{\lambda_{23\bar{4}\bar{5}}} + \frac{1}{\lambda_{125}} \right) + \frac{1}{\lambda_{134}\lambda_{2345}} \right] \\ &\quad + 4\lambda_2 \left[\left(\frac{1 + \beta^2}{2} + \frac{m^2}{\lambda_{13\bar{4}}\lambda_{134}} \right) \left(\frac{1}{\lambda_{13\bar{4}}} + \frac{1}{\lambda_{134}} \right) \right. \\ &\quad \left. + (d-2) \frac{\lambda_{1\bar{3}}}{s} \right]. \end{aligned} \quad (21)$$

The interaction coupling at second order is $g_f^{(1)} = g_S^2 C_F g_f^{(0)}$, where g_S is the strong coupling, $C_F = 4/3$ and the tree-level coupling $g_f^{(0)}$ is defined in Eq. (12).

The phase-space residues with three particles in the final state are generated from the expression

$$\begin{aligned} \mathcal{A}_D^{(3,f)}(1356) &= \frac{g_f^{(1)}}{x_{135}} \left[\frac{2}{\lambda_{125}\lambda_{1\bar{2}\bar{5}}\lambda_{134}\lambda_{13\bar{4}}} \left(s - \lambda_{125}\lambda_{1\bar{2}\bar{5}} \right. \right. \\ &\quad \left. \left. - \lambda_{134}\lambda_{13\bar{4}} - \frac{m^2(\lambda_{125}\lambda_{1\bar{2}\bar{5}} + \lambda_{134}\lambda_{13\bar{4}})^2}{\lambda_{125}\lambda_{1\bar{2}\bar{5}}\lambda_{134}\lambda_{13\bar{4}}} \right) \overline{|\mathcal{M}_{f \rightarrow q\bar{q}}^{(0)}|^2} \right. \\ &\quad \left. + (d-2) \left(\frac{\lambda_{134}\lambda_{13\bar{4}}}{\lambda_{125}\lambda_{1\bar{2}\bar{5}}} + \frac{\lambda_{125}\lambda_{1\bar{2}\bar{5}}}{\lambda_{134}\lambda_{13\bar{4}}} \right) + c_D^{(f)} \right], \\ c_D^{(H)} &= 2(d-2), \quad c_D^{(\gamma^*)} = 2(d-4). \end{aligned} \quad (22)$$

In this expression the final-state quark is labelled as 3 and the antiquark as 5. The exchange of indices in Eq. (18) accounts for the symmetric phase-space residues

$$\begin{aligned} \mathcal{A}_D^{(3,f)}(236) &= \mathcal{A}_D^{(3,f)}(456) \Big|_{(5 \leftrightarrow 2, 4 \leftrightarrow 3)}, \\ \mathcal{A}_D^{(3,f)}(1246) &= \mathcal{A}_D^{(3,f)}(1356) \Big|_{(5 \leftrightarrow 2, 4 \leftrightarrow 3)}. \end{aligned} \quad (23)$$

Before moving on to the UV renormalization of the phase-space residues in Eq. (19) and Eq. (20) let us comment on their IR and threshold singularities. Both expressions become singular at $\lambda_{13\bar{4}} \rightarrow 0$ and this singularity corresponds to a collinear singularity due to the collinear splitting $13 \rightarrow 4$, where the outgoing quark is labelled as 4, and the labels 1 and 3 denote the internal particles running in the loop. Since the energy of 4 is limited by energy conservation, the region in which the loop three-momentum ℓ_1 generates a collinear singularity is bounded [68]. Another collinear singularity occurs at $\lambda_{12\bar{5}} \rightarrow 0$ when the virtual gluon becomes collinear with the antiquark. If the quark and antiquark are massive, these collinear singularities are shadowed by their mass. Nevertheless, these terms integrate to a mass-dependent logarithm, which is potentially large. The soft singularity, corresponding to a soft virtual gluon, occurs at $\lambda_1 \rightarrow 0$.

Both soft and collinear singularities, or quasicollinear large logarithms for massive quarks, cancel locally with the tree-level phase-space residues presented in Eq. (22), which also diverge as, e.g., $1/\lambda_{13\bar{4}}$ where 1 and 3 are now external particles, and 4 is the parent parton of the collinear splitting. The local cancellation of soft, collinear and quasicollinear configurations ensures that the massless limit of a massive implementation is smooth [20] and, unlike the state-of-the-art approach, does not require a new calculation.

There is also the expected unitary threshold singularity occurring at $\lambda_{23\bar{4}\bar{5}} \rightarrow 0$ that generates the absorptive (imaginary) part of the loop amplitude. Threshold singularities are integrable but numerically challenging, and often require the implementation of a contour deformation over the integration domain [69–71] or other alternative methods [72, 73] to numerically stabilize the integrand. They are known to be one of the main limitations of numerical approaches and imply a compromise between accuracy and lengthy computer jobs. Threshold singularities are, however, absent in the sum of all the unitary phase-space residues because the kernel vacuum amplitude is free of this kind of singularities. This is one of the most remarkable properties of LTD causal unitarity.

III. LOCAL UV RENORMALISATION AND MASS RENORMALISATION SCHEME

The phase-space residues with loop remainders are to be renormalised locally by suitable UV counterterms. For this purpose we follow the procedure presented in detail in Refs. [20, 24]. First, we rescale all the on-shell energies involving the loop three-momentum ℓ_1 , i.e., by the replacement

$$\sqrt{\ell_{12}^2 - \imath 0} \rightarrow \sqrt{(\rho \ell_1 + \ell_2)^2 + (\rho^2 - 1)\mu_{UV}^2 - \imath 0}, \quad (24)$$

and then we expand the phase-space residues $\mathcal{A}_D^{(3,f)}(456)$ in Eq. (19) and Eq. (20) for $\rho \rightarrow \infty$. This expansion provides the most singular UV behaviour from which the UV counterterm is constructed. The scale μ_{UV} is interpreted as the renormalisation scale [18] in the sense that the UV counterterm suppresses all the energy modes of $\mathcal{A}_D^{(3,f)}(456)$ above μ_{UV} , and locally matches its UV behaviour at very high energies. The

UV counterterm renders the phase-space residue UV finite. Yet, it is also necessary to subtract subleading terms to deliver the expected results in, e.g., the $\overline{\text{MS}}$ renormalisation scheme, after setting the space-time dimensions to $d = 4$ in the integrand.

The UV counterterm for the Higgs boson decay reads

$$\mathcal{A}_{UV}^{(3,H)}(456) = \frac{g_H^{(1)}}{x_{45}} \left[\Delta Z_H^{(UV)} \overline{|\mathcal{M}_{H \rightarrow q\bar{q}}^{(0)}|^2} - \Delta Z_m^{(UV)} 8m^2 (1 + \beta^2) + \Delta_H^{(UV)} \right], \quad (25)$$

where

$$\Delta Z_H^{(UV)} = \frac{1}{4\lambda_{UV}^3} \left(c_H^{(UV)} - c_\gamma^{(UV)} + \frac{3\mu_{UV}^2}{2\lambda_{UV}^2} \right), \quad (26)$$

$$\Delta Z_m^{(UV)} = \frac{1}{4\lambda_{UV}^3} \left(c_H^{(UV)} - c_\gamma^{(UV)} + \frac{15\mu_{UV}^2}{2\lambda_{UV}^2} \right) \Big|_{\mu_{UV}=m}.$$

The coefficients $c_H^{(UV)} = d$ and $c_\gamma^{(UV)} = (d-2)/2$ were defined in Ref. [24] and $\lambda_{UV} = \sqrt{\ell_1^2 + \mu_{UV}^2 - \imath 0}$. The terms proportional to μ_{UV}^2 in Eq. (26) are UV subleading contribution that determine the renormalisation scheme. The function

$$\Delta_H^{(UV)} = \frac{c_\gamma^{(UV)}}{s\lambda_{UV}^3} \left(-\frac{3(\ell_1 \cdot \ell_2)^2}{\lambda_{UV}^2} + \ell_2^2 + 2\ell_1 \cdot \ell_2 \right) \times \overline{|\mathcal{M}_{H \rightarrow q\bar{q}}^{(0)}|^2}, \quad (27)$$

integrates to zero in d space-time dimensions and therefore has no effect, but its contribution is essential to suppress the singular UV angular behaviour at very high energies.

The integrated UV counterterm is

$$\int d\Phi_{\ell_1} \mathcal{A}_{UV}^{(3,H)}(456) \tilde{\Delta}_{456} = \frac{\pi}{s\beta} g_H^{(1)} \tilde{S}_\epsilon \left[\frac{\mu^{2\epsilon}}{\mu_{UV}^{2\epsilon}} \times \frac{3}{\epsilon} \overline{|\mathcal{M}_{H \rightarrow q\bar{q}}^{(0)}|^2} - \frac{\mu^{2\epsilon}}{m^{2\epsilon}} \left(\frac{3}{\epsilon} + 4 \right) 8m^2 (1 + \beta^2) \right], \quad (28)$$

where $\tilde{S}_\epsilon = (4\pi)^{\epsilon-2} \Gamma(1+\epsilon)$. An important comment is in order here. The on-shell renormalisation scheme is defined by imposing that the renormalised selfenergy and its derivative with respect to the external momentum vanish when the external particle is on shell. The second condition fixes the renormalisation of the wave function, and the first fixes the renormalisation of the mass. The result in Eq. (28) is consistent with the customary approach where the term proportional to the squared LO amplitude receives contributions from the UV renormalisation of the $H \rightarrow q\bar{q}$ interaction vertex, and the wave functions of the quark and antiquark. In other words, Eq. (25) locally renormalises the Yukawa coupling as it is expected from the standard approach:

$$y_q^0 \mu^\epsilon = y_q \mu_{UV}^\epsilon \left(1 - \frac{\alpha_S}{4\pi} C_F \frac{3}{\epsilon} + \mathcal{O}(\alpha_S^2) \right). \quad (29)$$

The vacuum amplitude correctly accounts for the derivative of the quark and antiquark selfenergies through the residues of

the corresponding squared Feynman propagators. However, it also generates a term proportional to the square of the mass. This term would not be considered in the state-of-the-art approach because the renormalised selfenergy is fixed to vanish on shell. The term $\Delta Z_m^{(\text{UV})}$ in Eq. (26) restores the mass renormalisation in the on-shell scheme when the renormalisation scale is identified with the quark mass itself, which introduces an interesting physical interpretation. Moreover, the mass renormalisation in other schemes, e.g., the $\overline{\text{MS}}$ scheme, would be achieved by modifying the subleading UV factors of $\Delta Z_m^{(\text{UV})}$.

In the case of an off-shell photon, the UV counterterm reads

$$\mathcal{A}_{\text{UV}}^{(3,\gamma^*)}(456) = \frac{g_{\gamma^*}^{(1)}}{x_{45}} \left[\Delta Z_m^{(\text{UV})}(-8m^2) \left(1 - \frac{\beta^2}{d-2} \right) + \Delta_{\gamma^*}^{(\text{UV})} \right], \quad (30)$$

where $\Delta Z_m^{(\text{UV})}$ is the same as in Eq. (26), and the function that integrates to zero is

$$\Delta_{\gamma^*}^{(\text{UV})} = \frac{c_{\gamma}^{(\text{UV})}}{s\lambda_{\text{UV}}^3} \left(-\frac{3(\ell_1 \cdot \ell_2)^2}{\lambda_{\text{UV}}^2} + \ell_2^2 + 2\ell_1 \cdot \ell_2 \right) \times \overline{|\mathcal{M}_{\gamma^* \rightarrow q\bar{q}}^{(0)}|^2} + \frac{3(2\ell_1 \cdot \ell_2)^2}{\lambda_{\text{UV}}^2} + \left(d-4 + \frac{3\mu_{\text{UV}}^2}{\lambda_{\text{UV}}^2} - \beta^2 \right) s, \quad (31)$$

such that

$$\int d\Phi_{\ell_1} \mathcal{A}_{\text{UV}}^{(3,\gamma^*)}(456) \tilde{\Delta}_{45\bar{6}} = \frac{\pi}{s\beta} g_{\gamma^*}^{(1)} \tilde{S}_\epsilon \times \frac{\mu^{2\epsilon}}{m^{2\epsilon}} \left(\frac{3}{\epsilon} + 4 \right) (-8m^2) \left(1 - \frac{\beta^2}{d-2} \right). \quad (32)$$

This result is consistent with the fact that conserved or partially conserved currents, such as the vector and axial currents, do not get renormalised. In other words, the UV counterterm in Eq. (30) renormalises the quark mass in the on-shell scheme, exactly as Eq. (25) does, but does not renormalise the wave function.

Summarising, the locally renormalised phase-space residue in Eq. (18) is then given by the four dimensional limit of the difference

$$\mathcal{A}_{\text{D}}^{(3,f,\text{R})}(456) = \left(\mathcal{A}_{\text{D}}^{(3,f)}(456) - \mathcal{A}_{\text{UV}}^{(3,f)}(456) \right) \Big|_{d=4}. \quad (33)$$

IV. A TOY DECAY RATE AT NNLO

We now consider the decay of a very heavy scalar into lighter or massless scalars at NNLO. Actually, we will not consider this decay in a realistic scalar theory, but rather in the simplified scenario generated by a single four-loop vacuum topology, which is shown in Fig. 2. This simplification contains all the necessary elements to illustrate LTD causal unitary at NNLO, while allowing us to explicitly describe the

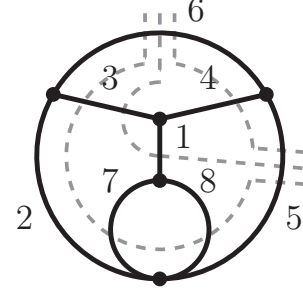


FIG. 2. Four-loop vacuum diagram generating the decay rate of a massive scalar particle at NNLO. The gray dashed lines represent phase-space residues.

two-loop, one-loop and tree-level phase-space residues with very compact expressions. Only the selfenergy-like insertion needs to be renormalised. With respect to the previous examples, which are defined by the set of momenta in Eq. (10), we now have two extra propagators with four-momenta

$$q_7 = \ell_4, \quad q_8 = \ell_4 + \ell_{12}, \quad (34)$$

and two extra independent integration variables, the modulus $|\ell_4|$ and the polar angle between the three-momenta ℓ_4 and ℓ_{12} . The NNLO contribution to the decay rate is

$$d\Gamma_{\Phi \rightarrow \phi\phi}^{(2)} = \frac{d\Phi_{\ell_1\ell_2\ell_4}}{2\sqrt{s}} \left[\left(\mathcal{A}_{\text{D}}^{(4,\Phi,\text{R})}(456) \tilde{\Delta}_{45\bar{6}} + \mathcal{A}_{\text{D}}^{(4,\Phi,\text{R})}(1356) \tilde{\Delta}_{135\bar{6}} + \mathcal{A}_{\text{D}}^{(4,\Phi)}(35678) \tilde{\Delta}_{35\bar{6}78} \right) + (5 \leftrightarrow 2, 4 \leftrightarrow 3) \right]. \quad (35)$$

The phase-space residue involving two-loop amplitudes is

$$\mathcal{A}_{\text{D}}^{(4,\Phi)}(456) = \frac{g_{\Phi}^{(2)} s^3}{x_{1234578}} \times \left[\frac{1}{\lambda_{134}} \left(L_{3478,2578}^{234\bar{5}} + L_{125,3478}^{2578} + L_{125,2578}^{178} \right) + \frac{1}{\lambda_{134}} \left(L_{2345,178}^{2578} + L_{2345,2578}^{3478} \right) + \frac{1}{\lambda_{125}} \left(L_{2578,178}^{134} + L_{2578,178}^{234\bar{5}} \right) + \frac{1}{\lambda_{125}} L_{2578,178}^{2345} + \frac{1}{\lambda_{178}} \left(L_{2345,2578}^{3478} + L_{2345,2578}^{3\bar{4}78} \right) \right], \quad (36)$$

with

$$L_{j,k}^i = \frac{1}{\lambda_i} \left(\frac{1}{\lambda_j} + \frac{1}{\lambda_k} \right). \quad (37)$$

There is another phase-space residue at one-loop

$$\mathcal{A}_{\text{D}}^{(4,\Phi)}(1356) = \frac{g_{\Phi}^{(2)} s^3}{x_{13578}} \left(\frac{1}{\lambda_{134}\lambda_{134}\lambda_{125}\lambda_{125}} \right) \times \left(\frac{1}{\lambda_{178}} + \frac{1}{\lambda_{178}} \right), \quad (38)$$

and the tree-level contribution

$$\mathcal{A}_D^{(4,\Phi)}(35678) = -\frac{g_\Phi^{(2)} s^3}{x_{3578}} \times \left(\frac{1}{\lambda_{3478} \lambda_{3478} \lambda_{2578} \lambda_{2578} \lambda_{178} \lambda_{178}} \right). \quad (39)$$

In addition, we should consider those phase-space residues that are obtained by exchanging the indices ($2 \leftrightarrow 5, 3 \leftrightarrow 4$), i.e. $\mathcal{A}_D^{(4,\Phi)}(236)$, $\mathcal{A}_D^{(4,\Phi)}(1246)$ and $\mathcal{A}_D^{(4,\Phi)}(24678)$. Notice that these expressions are the same regardless of whether the final-state scalars are massive or massless since the scalar masses are implicit in the on-shell energies.

It is then easy to realise how collinear and quasicollinear singularities cancel locally among different phase-space residues. For example, there are two double-collinear singularities at $\lambda_{13\bar{4}} \rightarrow 0$ and $\lambda_{\bar{1}78} \rightarrow 0$, respectively, which cancel out as

$$\begin{aligned} \lim_{\lambda_{13\bar{4}} \rightarrow 0} \left(\mathcal{A}_D^{(4,\Phi)}(456) \tilde{\Delta}_{45\bar{6}} + \mathcal{A}_D^{(4,\Phi)}(1356) \tilde{\Delta}_{135\bar{6}} \right) &= \mathcal{O}(\lambda_{13\bar{4}}^0), \\ \lim_{\lambda_{\bar{1}78} \rightarrow 0} \left(\mathcal{A}_D^{(4,\Phi)}(1356) \tilde{\Delta}_{135\bar{6}} + \mathcal{A}_D^{(4,\Phi)}(35678) \tilde{\Delta}_{356\bar{7}8} \right) &= \mathcal{O}(\lambda_{\bar{1}78}^0). \end{aligned} \quad (40)$$

When both double-collinear singularities occur simultaneously, which is equivalent to the limit $\lambda_{3\bar{4}78} \rightarrow 0$, a triple-collinear singularity emerges, and the three phase-space residues are needed to achieve a local cancellation

$$\lim_{\lambda_{3\bar{4}78} \rightarrow 0} \left(\mathcal{A}_D^{(4,\Phi)}(456) \tilde{\Delta}_{45\bar{6}} + \mathcal{A}_D^{(4,\Phi)}(1356) \tilde{\Delta}_{135\bar{6}} + \mathcal{A}_D^{(4,\Phi)}(35678) \tilde{\Delta}_{356\bar{7}8} \right) = \mathcal{O}(\lambda_{3\bar{4}78}^0). \quad (41)$$

Finally, a unitary threshold singularity arises at $\lambda_{23\bar{4}\bar{5}} \rightarrow 0$ that matches locally between $\mathcal{A}_D^{(4,\Phi)}(456)$ and $\mathcal{A}_D^{(4,\Phi)}(236)$.

The two- and one-loop phase-space residues need to be renormalised in the UV region. Following the same procedure explained above, the UV counterterms of these phase-space residues are given by

$$\begin{aligned} \mathcal{A}_{UV}^{(4,\Phi)}(456) &= \frac{g_\Phi^{(2)} s}{4\lambda_{UV}^3} \mathcal{A}_D^{(3,\Phi)}(456), \\ \mathcal{A}_{UV}^{(4,\Phi)}(1356) &= \frac{g_\Phi^{(2)} s}{4\lambda_{UV}^3} \mathcal{A}_D^{(3,\Phi)}(1356), \end{aligned} \quad (42)$$

respectively, where the UV on-shell energy is $\lambda_{UV} = \sqrt{\ell_4^2 + \mu_{UV}^2 - i0}$, and $\mathcal{A}_D^{(3,\Phi)}(456)$ and $\mathcal{A}_D^{(3,\Phi)}(1356)$ are the coupling-stripped phase-space residues to one less order

$$\begin{aligned} \mathcal{A}_D^{(3,\Phi)}(456) &= \frac{s^2}{x_{12345}} \left(L_{234\bar{5},125}^{13\bar{4}} + L_{234\bar{5},134}^{12\bar{5}} + L_{134,125}^{234\bar{5}} \right), \\ \mathcal{A}_D^{(3,\Phi)}(1356) &= \frac{s^2}{x_{135}} \left(\frac{1}{\lambda_{13\bar{4}} \lambda_{134} \lambda_{12\bar{5}} \lambda_{125}} \right). \end{aligned} \quad (43)$$

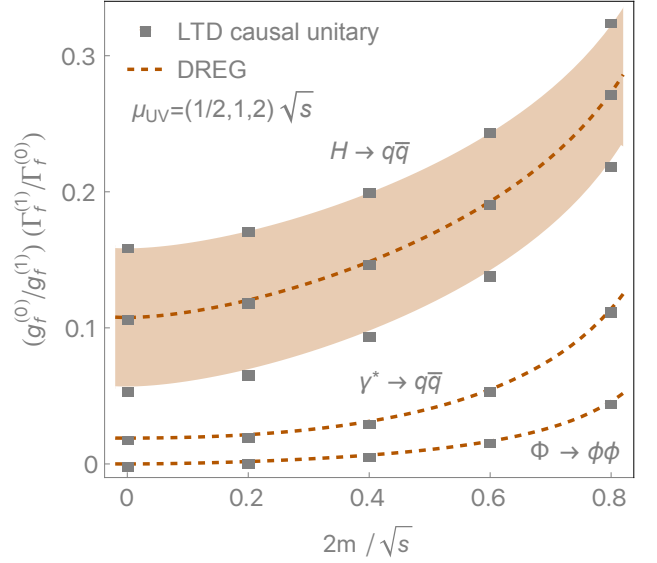


FIG. 3. Numerical implementation of LTD causal unitarity at NLO for the three decay processes $H \rightarrow q\bar{q}$, $\gamma^* \rightarrow q\bar{q}$ and $\Phi \rightarrow \phi\phi$ as a function of the final state mass.

For reference, the coupling-stripped phase-space residue at LO is dimensionless and is given by $\mathcal{A}_D^{(2,\Phi)}(456) = s/x_{45} = 1$, while

$$\begin{aligned} d\Gamma_{\Phi \rightarrow \phi\phi}^{(1)} &= \frac{d\Phi_{\ell_1 \ell_2}}{2\sqrt{s}} \left[\left(\mathcal{A}_D^{(3,\Phi)}(456) \tilde{\Delta}_{45\bar{6}} \right. \right. \\ &\quad \left. \left. + \mathcal{A}_D^{(3,\Phi)}(1356) \tilde{\Delta}_{135\bar{6}} \right) + (5 \leftrightarrow 2, 4 \leftrightarrow 3) \right]. \end{aligned} \quad (44)$$

V. NUMERICAL IMPLEMENTATION

With the expressions presented in the previous sections, we now introduce a numerical implementation directly in the three physical spatial dimensions, $d - 1 = 3$, since IR singularities cancel locally among phase-space residues and the local UV counterterm properly accounts for the singular UV behaviour. Unitary threshold singularities also match locally in the sum of the loop phase-space residues rendering the integrand well behaved across thresholds. To this end, we must consider the constraints introduced by energy conservation, which are encoded by the functions $\tilde{\Delta}_{i_1 \dots i_n \bar{6}}$ in Eq. (15), Eq. (18) and Eq. (35).

The phase-space energy function $\tilde{\Delta}_{45\bar{6}}$ only involves the ℓ_2 and ℓ_3 loop momenta and leaves ℓ_1 unconstrained. Since at the centre-of-mass frame we set $\ell_3 = \mathbf{0}$, then $\tilde{\Delta}_{45\bar{6}}$ fixes the modulus of ℓ_2 and leaves the angular dependence unconstrained. Conversely, $\tilde{\Delta}_{23\bar{6}}$ fixes the modulus of ℓ_1 . This is the expected constraint of a two-body phase space. The phase-space energy functions $\tilde{\Delta}_{135\bar{6}}$ and $\tilde{\Delta}_{124\bar{6}}$ involve the three loop momenta. Since all the loop momenta are now bounded by $q_{6,0}^{(+)} = \sqrt{s - i0}$, then the integration domain is restricted

to a compact region of the phase space, corresponding to a three-body phase space.

If p_1 and p_2 are the momenta of the quark and the antiquark, respectively, in the final-state with two particles, and p'_1, p'_2 and p'_3 are the momenta of the quark, antiquark and gluon in the final state with three particles, the following mappings apply

$$\begin{aligned} p_a(6) &\rightarrow p_1(4) + p_2(\bar{5}), \\ p_a(6) &\rightarrow p_1(\bar{3}) + p_2(2), \\ p_a(6) &\rightarrow p'_1(4) + p'_2(2) + p'_3(\bar{1}), \\ p_a(6) &\rightarrow p'_1(\bar{3}) + p'_2(\bar{5}) + p'_3(1), \end{aligned} \quad (45)$$

where the mapping is interpreted in the following sense

$$p_s(i) : p_s^\mu = (\sqrt{\mathbf{q}_i^2 + m_i^2} - i0, \mathbf{q}_i), \quad (46)$$

and the on-shell energies are

$$\begin{aligned} q_{1,0}^{(+)} &= \sqrt{\ell_{12}^2 - i0}, \\ q_{2,0}^{(+)} &= q_{3,0}^{(+)} = \sqrt{\ell_1^2 + m^2 - i0}, \\ q_{4,0}^{(+)} &= q_{5,0}^{(+)} = \sqrt{\ell_2^2 + m^2 - i0}. \end{aligned} \quad (47)$$

As expected, there are five independent integration variables considering two modulus, four angles and one energy conservation constraint. Nevertheless, assuming the decaying particle to be at rest the number of effective independent variables is two.

The phase-space energy function $\tilde{\Delta}_{35\bar{6}78}$ in Eq. (35) and its symmetric counterpart $\tilde{\Delta}_{24\bar{6}78}$ introduce a dependence in the ℓ_4 loop momentum, and therefore two additional independent integration variables. We should also consider final-states with four external particles and the mappings

$$\begin{aligned} p_a(6) &\rightarrow p''_1(4) + p''_2(2) + p''_4(\bar{7}) + p''_5(\bar{8}), \\ p_a(6) &\rightarrow p''_1(\bar{3}) + p''_2(\bar{5}) + p''_4(7) + p''_5(8), \end{aligned} \quad (48)$$

with

$$\begin{aligned} q_{7,0}^{(+)} &= \sqrt{\ell_4^2 + m^2 - i0}, \\ q_{8,0}^{(+)} &= \sqrt{(\ell_4 + \ell_{12})^2 + m^2 - i0}. \end{aligned} \quad (49)$$

The numerical implementation is quite stable, in particular due to the absence of unitary threshold singularities. The numerical results obtained for the NLO contribution to the decay rates, normalised to the LO total decay rate, are presented in Fig. 3, where they are compared with state-of-the-art DREG analytical expressions. The agreement shown is excellent. Only $H \rightarrow q\bar{q}$ exhibits a dependence on the renormalisation scale μ_{UV} because the vector current of the photon decay is UV protected and the scalar decay is UV finite at NLO.

In Fig. 4 and Fig. 5, we illustrate the integrand behaviour of the different phase-space residues and their sum across a unitary threshold singularity and in collinear configurations,

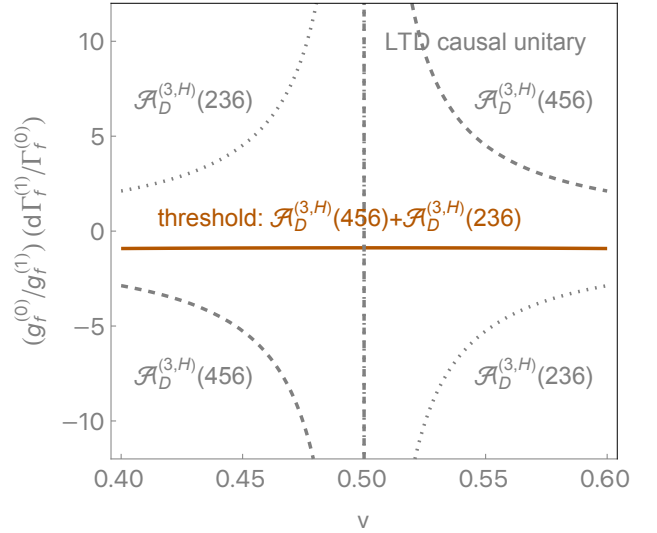


FIG. 4. Unintegrated decay rate across a unitary threshold singularity as a function of the angular variable. The sum over the one-loop phase-space residues is flat.

respectively. We can clearly observe how the different phase-space residues are singular, but their sum provides a flat integrand. The phase-space residues shown in Fig. 4 and Fig. 5 correspond to $H \rightarrow q\bar{q}$. Similar results are obtained for the other two processes.

The local cancellation of collinear singularities at NNLO is illustrated in Fig. 6 for the toy model described in Section IV. We have fixed the angular variable that defines the collinearity of particles 7 and 8 to $v_4 = 10^{-2}$. We can observe that for large values of the other angular variable, v , the cancellation occurs mostly between $\mathcal{A}_D^{(4,\Phi)}(1356)$ and $\mathcal{A}_D^{(4,\Phi)}(35678)$, which corresponds to the local cancellation of the double-collinear singularity at $\lambda_{178} \rightarrow 0$ according to Eq. (40). At very small angles, $v < v_4$, instead $\mathcal{A}_D^{(4,\Phi)}(456)$ becomes much more singular than $\mathcal{A}_D^{(4,\Phi)}(35678)$, reflecting the dominance of the emergent triple-collinear configuration, and the participation of the three phase-space residues is necessary for the local cancellation of the overlapping collinear singularities, according to Eq. (41).

Comparing Fig. 6 and Fig. 5, we also observe that the local cancellation of collinear singularities is equally effective at NLO and NNLO, although the scale of the individual singularities is, as expected, much larger at NNLO.

VI. CONCLUSIONS

We have presented the first proof-of-concept implementation of LTD causal unitary [1] to decay processes at higher perturbative orders. The processes chosen are such that all the benefits of the method are clearly visible in a lightweight manner. Specifically, the central and novel ingredient of LTD causal unitary is the use of a multiloop vacuum amplitude in

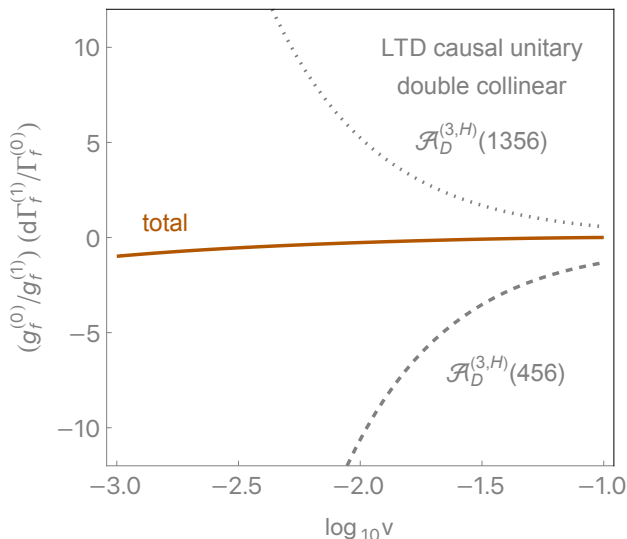


FIG. 5. Local cancellation of collinear singularities at NLO between phase-space residues with different numbers of final-state particles.

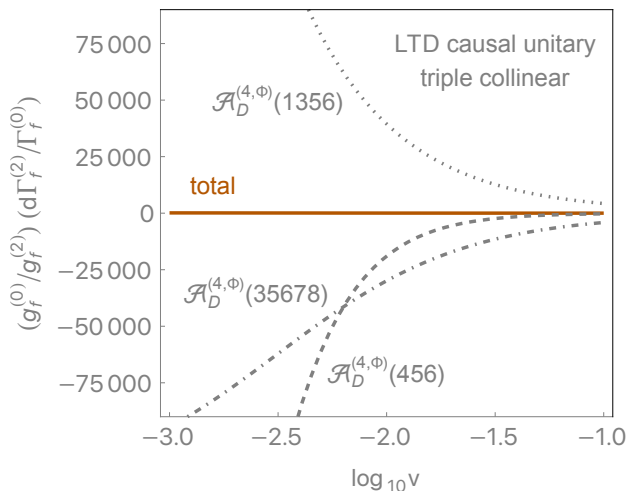


FIG. 6. Local cancellation of collinear singularities at NNLO between phase-space residues with different numbers of final-state particles.

the LTD representation as a kernel of all the final states contributing to the decay process. The LTD representation of the vacuum amplitude, which is manifestly causal, coherently encodes these final states as residues on causal propagators that depend on linear combinations of the on-shell energies of the internal propagators, once certain on-shell energies identified with the incoming particles are analytically continued to negative values.

LTD causal unitary ensures the local cancellation of soft and collinear or quasicollinear singularities to all orders in perturbation theory through the unitary sum of the phase-space residues, while the renormalisation of UV singularities is achieved through suitable UV local counterterms. The use of vacuum amplitudes as a kernel incorporates the wave-

function renormalisation of external particles in a well-defined approach that is free from mathematical ambiguities. The mass renormalisation is also physically interpreted as a function of a proper renormalisation scale.

Concerning unitary threshold singularities, which typically represent an overwhelming obstacle in numerical implementations, LTD causal unitary provides an efficient solution leading to flat integrands across thresholds, as the potential singularities match between phase-space residues with the same number of final-state particles. This property, which is a natural consequence of using a vacuum amplitude as a kernel, represents a clear advantage over other methods.

The local cancellation of singularities at NLO and NNLO has been illustrated with selected decay processes. The total decay rates at NLO have been obtained with LTD causal unitary and have been compared with state-of-the-art DREG analytical expressions, showing a perfect agreement. The transition from a massive to a massless implementation, as already observed in [20], is smooth. The numerical implementation in LTD causal unitary is quite stable and leads to accurate results with minimal CPU resources.

The results presented in this paper constitute a solid confirmation of the unique capabilities and advantages of LTD causal unitary at higher perturbative orders, in addition to successfully addressing the original motivation and path initiated with the seminal works on the loop-tree duality [74–76]. A proof-of-concept implementation for scattering processes that require a local subtraction of initial-state collinear singularities, as well as more complex and well-motivated phenomenological analysis with LTD causal unitary for scattering and decay processes at high-energy colliders, will be presented in forthcoming publications.

ACKNOWLEDGEMENTS

This work is dedicated to the memory of Stefano Catani, who always inspired us in the development of this research line, and very touching during the Workshop *Theory Challenges in the Precision Era of the Large Hadron Collider* held at the Galileo Galilei Institute (Firenze) in September 2023. This work is supported by the Spanish Government (Agencia Estatal de Investigación MCIN/AEI/10.13039/501100011033) Grants No. PID2020-114473GB-I00 and PID2022-141910NB-I00, and Generalitat Valenciana Grant No. PROMETEO/2021/071. AERO is supported by the Spanish Government (PRE2018-085925). DFRE and JML are supported by Generalitat Valenciana (CIGRIS/2022/145 and ACIF/2021/219). PKD is supported by European Commission MSCA Action COLLINER-FRACTURE, Grant Agreement No. 101108573. SRU and RJHP are funded by CONAHCyT through Project No. 320856 (Paradigmas y Controversias de la Ciencia 2022), Ciencia de Frontera 2021-2042 and Sistema Nacional de Investigadores. LC is supported by Generalitat Valenciana GenT Excellence Programme (CIDEAGENT/2020/011) and ILINK22045. GS is partially supported by EU Horizon 2020 research and innovation programme STRONG-2020 project

under Grant Agreement No. 824093 and H2020-MSCA-COFUND USAL4EXCELLENCE-PROOPI-391 project under Grant Agreement No 101034371. WJT is supported by the Leverhulme Trust, LIP-2021-01.

Appendix A: The phase space

Our representation of the phase space for m particles in the final state is derived from the standard expression

$$d\Phi_m = \mu^{d-4} (2\pi)^d \delta^{(d)} \left(\sum_{i=1}^m p_i - p_{ab} \right) \prod_{i=1}^m \frac{\mu^{4-d} d^{d-1} p_i}{(2\pi)^{d-1} 2E_i}, \quad (\text{A1})$$

where $p_{ab} = p_a + p_b$ stands for the sum of initial-state momenta. Inspired by the LTD representation of multiloop amplitudes, we first define

$$d\Phi_{\mathbf{p}_i} = \mu^{4-d} \frac{d^{d-1} p_i}{(2\pi)^{d-1}}, \quad (\text{A2})$$

which is typically parametrised as

$$d\Phi_{\mathbf{p}_i} = \frac{\mu^{2\epsilon}}{(2\pi)^{d-1}} (\mathbf{p}_i^2)^{1-\epsilon} d|\mathbf{p}_i| d\Omega_i^{(d-2)},$$

$$d\Omega_i^{(d-2)} = \frac{(4\pi)^{1-\epsilon}}{\Gamma(1-\epsilon)} (v_i(1-v_i))^{-\epsilon} dv_i. \quad (\text{A3})$$

Then, we identify $E_i \rightarrow p_{i,0}^{(+)} = \sqrt{\mathbf{p}_i^2 + m_i^2} - i0$ as the on-shell energies, to rewrite the phase space as

$$d\Phi_m = \mu^{d-4} (2\pi)^{d-1} \delta^{(d-1)} \left(\sum_{i=1}^m \mathbf{p}_i - \mathbf{p}_{ab} \right) \times \frac{\tilde{\Delta}_{1\dots m\bar{a}\bar{b}}}{x_{1\dots m}} d\Phi_{\mathbf{p}_1, \dots, \mathbf{p}_m}, \quad (\text{A4})$$

where $x_{1\dots m} = \prod_{i=1}^m 2p_{i,0}^{(+)}$ is the product of all the on-shell energies of the final-state particles. The energy-conservation Dirac delta function is specifically given by

$$\tilde{\Delta}_{1\dots m\bar{a}\bar{b}} = 2\pi \delta(\lambda_{1\dots m\bar{a}\bar{b}}), \quad (\text{A5})$$

where

$$\lambda_{1\dots m\bar{a}\bar{b}} = \sum_{i=1}^m p_{i,0}^{(+)} - p_{a,0}^{(+)} - p_{b,0}^{(+)}. \quad (\text{A6})$$

-
- [1] S. Ramírez-Urbe, P. K. Dhani, G. F. R. Sborlini, and G. Rodrigo, Rewording theoretical predictions at colliders with vacuum amplitudes, (2024), arXiv:2404. [hep-ph].
 - [2] J. J. Aguilera-Verdugo, F. Driencourt-Mangin, R. J. Hernández-Pinto, J. Plenter, S. Ramírez-Urbe, A. E. Rentería Olivo, G. Rodrigo, G. F. R. Sborlini, W. J. Torres Bobadilla, and S. Tracz, Open Loop Amplitudes and Causality to All Orders and Powers from the Loop-Tree Duality, Phys. Rev. Lett. **124**, 211602 (2020), arXiv:2001.03564 [hep-ph].
 - [3] J. J. Aguilera-Verdugo, R. J. Hernández-Pinto, S. Ramírez-Urbe, A. E. Rentería-Olivo, G. Rodrigo, G. F. R. Sborlini, and W. J. Torres Bobadilla, Manifestly Causal Scattering Amplitudes, Snowmass LoI (August 2020).
 - [4] J. J. Aguilera-Verdugo, R. J. Hernandez-Pinto, G. Rodrigo, G. F. R. Sborlini, and W. J. Torres Bobadilla, Causal representation of multi-loop Feynman integrands within the loop-tree duality, JHEP **01**, 069, arXiv:2006.11217 [hep-ph].
 - [5] S. Ramírez-Urbe, R. J. Hernández-Pinto, G. Rodrigo, G. F. R. Sborlini, and W. J. Torres Bobadilla, Universal opening of four-loop scattering amplitudes to trees, JHEP **04**, 129, arXiv:2006.13818 [hep-ph].
 - [6] J. Jesús Aguilera-Verdugo, R. J. Hernández-Pinto, G. Rodrigo, G. F. R. Sborlini, and W. J. Torres Bobadilla, Mathematical properties of nested residues and their application to multi-loop scattering amplitudes, JHEP **02**, 112, arXiv:2010.12971 [hep-ph].
 - [7] G. F. R. Sborlini, Geometrical approach to causality in multiloop amplitudes, Phys. Rev. D **104**, 036014 (2021), arXiv:2102.05062 [hep-ph].
 - [8] W. J. Torres Bobadilla, Loop-tree duality from vertices and edges, JHEP **04**, 183, arXiv:2102.05048 [hep-ph].
 - [9] W. J. T. Bobadilla, Lotty – The loop-tree duality automation, Eur. Phys. J. C **81**, 514 (2021), arXiv:2103.09237 [hep-ph].
 - [10] J. de Jesús Aguilera-Verdugo *et al.*, A Stroll through the Loop-Tree Duality, Symmetry **13**, 1029 (2021), arXiv:2104.14621 [hep-ph].
 - [11] S. Ramírez-Urbe, A. E. Rentería-Olivo, G. Rodrigo, G. F. R. Sborlini, and L. Vale Silva, Quantum algorithm for Feynman loop integrals, JHEP **05**, 100, arXiv:2105.08703 [hep-ph].
 - [12] P. Benincasa and W. J. T. Bobadilla, Physical representations for scattering amplitudes and the wavefunction of the universe, SciPost Phys. **12**, 192 (2022), arXiv:2112.09028 [hep-th].
 - [13] S. Kromin, N. Schwanemann, and S. Weinzierl, Amplitudes within causal loop-tree duality, Phys. Rev. D **106**, 076006 (2022), arXiv:2208.01060 [hep-th].
 - [14] G. Clemente, A. Crippa, K. Jansen, S. Ramírez-Urbe, A. E. Rentería-Olivo, G. Rodrigo, G. F. R. Sborlini, and L. Vale Silva, Variational quantum eigensolver for causal loop Feynman diagrams and directed acyclic graphs, Phys. Rev. D **108**, 096035 (2023), arXiv:2210.13240 [hep-ph].
 - [15] J. J. M. de Lejarza, L. Cieri, M. Grossi, S. Vallecorsa, and G. Rodrigo, Loop Feynman integration on a quantum computer, (2024), arXiv:2401.03023 [hep-ph].
 - [16] J. Rios-Sanchez and G. Sborlini, Towards multiloop local renormalization within Causal Loop-Tree Duality, (2024), arXiv:2402.13995 [hep-th].
 - [17] S. Ramírez-Urbe, A. E. Rentería-Olivo, and G. Rodrigo, Quantum querying based on multicontrolled Toffoli gates for causal Feynman loop configurations and directed acyclic graphs,

- (2024), arXiv:2404.03544 [quant-ph].
- [18] R. J. Hernandez-Pinto, G. F. R. Sborlini, and G. Rodrigo, Towards gauge theories in four dimensions, *JHEP* **02**, 044, arXiv:1506.04617 [hep-ph].
- [19] G. F. R. Sborlini, F. Driencourt-Mangin, R. Hernandez-Pinto, and G. Rodrigo, Four-dimensional unsubtraction from the loop-tree duality, *JHEP* **08**, 160, arXiv:1604.06699 [hep-ph].
- [20] G. F. R. Sborlini, F. Driencourt-Mangin, and G. Rodrigo, Four-dimensional unsubtraction with massive particles, *JHEP* **10**, 162, arXiv:1608.01584 [hep-ph].
- [21] R. M. Prisco and F. Tramontano, Dual subtractions, *JHEP* **06**, 089, arXiv:2012.05012 [hep-ph].
- [22] F. Driencourt-Mangin, G. Rodrigo, and G. F. R. Sborlini, Universal dual amplitudes and asymptotic expansions for $gg \rightarrow H$ and $H \rightarrow \gamma\gamma$ in four dimensions, *Eur. Phys. J. C* **78**, 231 (2018), arXiv:1702.07581 [hep-ph].
- [23] F. Driencourt-Mangin, *Four-dimensional representation of scattering amplitudes and physical observables through the application of the Loop-Tree Duality theorem*, Ph.D. thesis, U. Valencia (main) (2019), arXiv:1907.12450 [hep-ph].
- [24] F. Driencourt-Mangin, G. Rodrigo, G. F. R. Sborlini, and W. J. Torres Bobadilla, Universal four-dimensional representation of $H \rightarrow \gamma\gamma$ at two loops through the Loop-Tree Duality, *JHEP* **02**, 143, arXiv:1901.09853 [hep-ph].
- [25] F. Driencourt-Mangin, G. Rodrigo, G. F. R. Sborlini, and W. J. Torres Bobadilla, Interplay between the loop-tree duality and helicity amplitudes, *Phys. Rev. D* **105**, 016012 (2022), arXiv:1911.11125 [hep-ph].
- [26] Z. Kunszt and D. E. Soper, Calculation of jet cross-sections in hadron collisions at order α_s^3 , *Phys. Rev. D* **46**, 192 (1992).
- [27] S. Frixione, Z. Kunszt, and A. Signer, Three jet cross-sections to next-to-leading order, *Nucl. Phys. B* **467**, 399 (1996), arXiv:hep-ph/9512328.
- [28] S. Catani and M. H. Seymour, The Dipole formalism for the calculation of QCD jet cross-sections at next-to-leading order, *Phys. Lett. B* **378**, 287 (1996), arXiv:hep-ph/9602277.
- [29] S. Catani and M. H. Seymour, A General algorithm for calculating jet cross-sections in NLO QCD, *Nucl. Phys. B* **485**, 291 (1997), [Erratum: *Nucl.Phys.B* 510, 503–504 (1998)], arXiv:hep-ph/9605323.
- [30] S. Catani, D. de Florian, and M. Grazzini, Universality of nonleading logarithmic contributions in transverse momentum distributions, *Nucl. Phys. B* **596**, 299 (2001), arXiv:hep-ph/0008184.
- [31] Z. Nagy and D. E. Soper, General subtraction method for numerical calculation of one loop QCD matrix elements, *JHEP* **09**, 055, arXiv:hep-ph/0308127.
- [32] S. Weinzierl, Subtraction terms at NNLO, *JHEP* **03**, 062, arXiv:hep-ph/0302180.
- [33] S. Frixione and M. Grazzini, Subtraction at NNLO, *JHEP* **06**, 010, arXiv:hep-ph/0411399.
- [34] W. B. Kilgore, Subtraction terms for hadronic production processes at next-to-next-to-leading order, *Phys. Rev. D* **70**, 031501 (2004), arXiv:hep-ph/0403128.
- [35] S. Catani and M. Grazzini, An NNLO subtraction formalism in hadron collisions and its application to Higgs boson production at the LHC, *Phys. Rev. Lett.* **98**, 222002 (2007), arXiv:hep-ph/0703012.
- [36] S. Catani, L. Cieri, D. de Florian, G. Ferrera, and M. Grazzini, Universality of transverse-momentum resummation and hard factors at the NNLO, *Nucl. Phys. B* **881**, 414 (2014), arXiv:1311.1654 [hep-ph].
- [37] A. Gehrmann-De Ridder, T. Gehrmann, and E. W. N. Glover, Antenna subtraction at NNLO, *JHEP* **09**, 056, arXiv:hep-ph/0505111.
- [38] A. Gehrmann-De Ridder, T. Gehrmann, and M. Ritzmann, Antenna subtraction at NNLO with hadronic initial states: double real initial-initial configurations, *JHEP* **10**, 047, arXiv:1207.5779 [hep-ph].
- [39] A. Daleo, T. Gehrmann, and D. Maitre, Antenna subtraction with hadronic initial states, *JHEP* **04**, 016, arXiv:hep-ph/0612257.
- [40] G. Somogyi, Z. Trocsanyi, and V. Del Duca, A Subtraction scheme for computing QCD jet cross sections at NNLO: Regularization of doubly-real emissions, *JHEP* **01**, 070, arXiv:hep-ph/0609042.
- [41] G. Somogyi and Z. Trocsanyi, A Subtraction scheme for computing QCD jet cross sections at NNLO: Regularization of real-virtual emission, *JHEP* **01**, 052, arXiv:hep-ph/0609043.
- [42] G. Somogyi and Z. Trocsanyi, A Subtraction scheme for computing QCD jet cross sections at NNLO: Integrating the subtraction terms. I., *JHEP* **08**, 042, arXiv:0807.0509 [hep-ph].
- [43] G. Somogyi, Subtraction with hadronic initial states at NLO: An NNLO-compatible scheme, *JHEP* **05**, 016, arXiv:0903.1218 [hep-ph].
- [44] P. Bolzoni, G. Somogyi, and Z. Trocsanyi, A subtraction scheme for computing QCD jet cross sections at NNLO: integrating the iterated singly-unresolved subtraction terms, *JHEP* **01**, 059, arXiv:1011.1909 [hep-ph].
- [45] T. Gleisberg and F. Krauss, Automating dipole subtraction for QCD NLO calculations, *Eur. Phys. J. C* **53**, 501 (2008), arXiv:0709.2881 [hep-ph].
- [46] M. Czakon, A novel subtraction scheme for double-real radiation at NNLO, *Phys. Lett. B* **693**, 259 (2010), arXiv:1005.0274 [hep-ph].
- [47] M. Czakon and D. Heymes, Four-dimensional formulation of the sector-improved residue subtraction scheme, *Nucl. Phys. B* **890**, 152 (2014), arXiv:1408.2500 [hep-ph].
- [48] G. Bevilacqua, M. Czakon, M. Kubocz, and M. Worek, Complete Nagy-Soper subtraction for next-to-leading order calculations in QCD, *JHEP* **10**, 204, arXiv:1308.5605 [hep-ph].
- [49] E. W. Nigel Glover and J. Pires, Antenna subtraction for gluon scattering at NNLO, *JHEP* **06**, 096, arXiv:1003.2824 [hep-ph].
- [50] J. Currie, E. W. N. Glover, and S. Wells, Infrared Structure at NNLO Using Antenna Subtraction, *JHEP* **04**, 066, arXiv:1301.4693 [hep-ph].
- [51] R. Bonciani, S. Catani, M. Grazzini, H. Sargsyan, and A. Torre, The q_T subtraction method for top quark production at hadron colliders, *Eur. Phys. J. C* **75**, 581 (2015), arXiv:1508.03585 [hep-ph].
- [52] J. Gaunt, M. Stahlhofen, F. J. Tackmann, and J. R. Walsh, N-jettiness Subtractions for NNLO QCD Calculations, *JHEP* **09**, 058, arXiv:1505.04794 [hep-ph].
- [53] R. Boughezal, A. Gehrmann-De Ridder, and M. Ritzmann, Antenna subtraction at NNLO with hadronic initial states: double real radiation for initial-initial configurations with two quark flavours, *JHEP* **02**, 098, arXiv:1011.6631 [hep-ph].
- [54] R. Boughezal, K. Melnikov, and F. Petriello, A subtraction scheme for NNLO computations, *Phys. Rev. D* **85**, 034025 (2012), arXiv:1111.7041 [hep-ph].
- [55] R. Boughezal, F. Caola, K. Melnikov, F. Petriello, and M. Schulze, Higgs boson production in association with a jet at next-to-next-to-leading order, *Phys. Rev. Lett.* **115**, 082003 (2015), arXiv:1504.07922 [hep-ph].
- [56] V. Del Duca, C. Duhr, A. Kardos, G. Somogyi, Z. Szőr, Z. Trócsányi, and Z. Tulipánt, Jet production in the CoLoR-

- FulNNLO method: event shapes in electron-positron collisions, Phys. Rev. D **94**, 074019 (2016), arXiv:1606.03453 [hep-ph].
- [57] L. Magnea, E. Maina, G. Pelliccioli, C. Signorile-Signorile, P. Torrielli, and S. Uccirati, Local analytic sector subtraction at NNLO, JHEP **12**, 107, [Erratum: JHEP 06, 013 (2019)], arXiv:1806.09570 [hep-ph].
- [58] L. Magnea, E. Maina, G. Pelliccioli, C. Signorile-Signorile, P. Torrielli, and S. Uccirati, Factorisation and Subtraction beyond NLO, JHEP **12**, 062, arXiv:1809.05444 [hep-ph].
- [59] F. Caola, K. Melnikov, and R. Röntsch, Analytic results for color-singlet production at NNLO QCD with the nested soft-collinear subtraction scheme, Eur. Phys. J. C **79**, 386 (2019), arXiv:1902.02081 [hep-ph].
- [60] L. Buonocore, M. Grazzini, and F. Tramontano, The q_T subtraction method: electroweak corrections and power suppressed contributions, Eur. Phys. J. C **80**, 254 (2020), arXiv:1911.10166 [hep-ph].
- [61] M. Delto and K. Melnikov, Integrated triple-collinear counterterms for the nested soft-collinear subtraction scheme, JHEP **05**, 148, arXiv:1901.05213 [hep-ph].
- [62] T. Engel, A. Signer, and Y. Ulrich, A subtraction scheme for massive QED, JHEP **01**, 085, arXiv:1909.10244 [hep-ph].
- [63] K. Asteriadis, F. Caola, K. Melnikov, and R. Röntsch, Analytic results for deep-inelastic scattering at NNLO QCD with the nested soft-collinear subtraction scheme, Eur. Phys. J. C **80**, 8 (2020), arXiv:1910.13761 [hep-ph].
- [64] L. Cieri, D. de Florian, M. Der, and J. Mazzitelli, Mixed QCD \otimes QED corrections to exclusive Drell Yan production using the q_T -subtraction method, JHEP **09**, 155, arXiv:2005.01315 [hep-ph].
- [65] W. J. Torres Bobadilla *et al.*, May the four be with you: Novel IR-subtraction methods to tackle NNLO calculations, Eur. Phys. J. C **81**, 250 (2021), arXiv:2012.02567 [hep-ph].
- [66] G. Bertolotti, L. Magnea, G. Pelliccioli, A. Ratti, C. Signorile-Signorile, P. Torrielli, and S. Uccirati, NNLO subtraction for any massless final state: a complete analytic expression, JHEP **07**, 140, arXiv:2212.11190 [hep-ph].
- [67] F. Devoto, K. Melnikov, R. Röntsch, C. Signorile-Signorile, and D. M. Tagliabue, A fresh look at the nested soft-collinear subtraction scheme: NNLO QCD corrections to N-gluon final states in $q\bar{q}$ annihilation, JHEP **02**, 016, arXiv:2310.17598 [hep-ph].
- [68] S. Buchta, G. Chachamis, P. Draggiotis, I. Malamos, and G. Rodrigo, On the singular behaviour of scattering amplitudes in quantum field theory, JHEP **11**, 014, arXiv:1405.7850 [hep-ph].
- [69] S. Becker, C. Reuschle, and S. Weinzierl, Numerical NLO QCD calculations, JHEP **12**, 013, arXiv:1010.4187 [hep-ph].
- [70] S. Buchta, G. Chachamis, P. Draggiotis, and G. Rodrigo, Numerical implementation of the loop–tree duality method, Eur. Phys. J. C **77**, 274 (2017), arXiv:1510.00187 [hep-ph].
- [71] Z. Capatti, V. Hirschi, D. Kermanschah, A. Pelloni, and B. Ruijl, Numerical Loop-Tree Duality: contour deformation and subtraction, JHEP **04**, 096, arXiv:1912.09291 [hep-ph].
- [72] R. Pittau and B. Webber, Direct numerical evaluation of multi-loop integrals without contour deformation, Eur. Phys. J. C **82**, 55 (2022), arXiv:2110.12885 [hep-ph].
- [73] D. Kermanschah, Numerical integration of loop integrals through local cancellation of threshold singularities, JHEP **01**, 151, arXiv:2110.06869 [hep-ph].
- [74] S. Catani, T. Gleisberg, F. Krauss, G. Rodrigo, and J.-C. Winter, From loops to trees by-passing Feynman’s theorem, JHEP **09**, 065, arXiv:0804.3170 [hep-ph].
- [75] I. Bierenbaum, S. Catani, P. Draggiotis, and G. Rodrigo, A Tree-Loop Duality Relation at Two Loops and Beyond, JHEP **10**, 073, arXiv:1007.0194 [hep-ph].
- [76] I. Bierenbaum, S. Buchta, P. Draggiotis, I. Malamos, and G. Rodrigo, Tree-Loop Duality Relation beyond simple poles, JHEP **03**, 025, arXiv:1211.5048 [hep-ph].